Oncogene (2009) 28, 412–421

www.nature.com/onc

ORIGINAL ARTICLE

The α-receptor for platelet-derived growth factor as a target for antibody-mediated inhibition of skeletal metastases from prostate cancer cells

MR Russell[1,4], WL Jamieson[1,4], NG Dolloff[1,3] and A Fatatis[1,2]

[1]*Department of Pharmacology and Physiology, Drexel University College of Medicine, Philadelphia, PA, USA and* [2]*Department of Pathology and Laboratory Medicine, Drexel University College of Medicine, Philadelphia, PA, USA*

Bone resorption by osteoclasts is thought to promote the proliferation of prostate cancer cells disseminated to the skeleton (Mundy, 2002). Using a mouse model of experimental metastasis, we found that although late-stage metastatic tumors were indeed surrounded by osteoclasts, these cells were spatially unrelated to the small foci of cancer cells in early-stage metastases. This is the first evidence that survival and growth of disseminated prostate cancer cells immediately after their extravasation may not depend on osteoclast involvement. Interestingly, prostate cancer cells expressing the α-receptor for platelet-derived growth factor (PDGFRα) progress during early-stages of skeletal dissemination, whereas cells expressing lower levels or lacking this receptor fail to survive after extravasation in the bone marrow. However, non-metastatic cells acquire bone-metastatic potential upon ectopic overexpression of PDGFRα. Finally, functional blockade of human PDGFRα on prostate cancer cells utilizing a novel humanized monoclonal antibody—soon to undergo phase-II clinical trials—significantly impairs the establishment of early skeletal metastases. In conclusion, our results strongly implicate PDGFRα in prostate cancer bone tropism through its promotion of survival and progression of early-metastatic foci, providing ground for therapeutic strategies aimed at preventing or containing the initial progression of skeletal metastases in patients affected by prostate adenocarcinoma.
Oncogene (2009) **28,** 412–421; doi:10.1038/onc.2008.390; published online 13 October 2008

Keywords: skeletal metastasis; prostate adenocarcinoma; PDGFRα

Correspondence: Dr A Fatatis, Department of Pharmacology and Physiology, Drexel University College of Medicine, 245 N. 15th Street, New College Building MS488, Philadelphia, PA 19102, USA.
E-mail: afatatis@drexelmed.edu
[3]Current address: Department of Medicine, University of Pennsylvania, Philadelphia, PA 19104, USA.
[4]MR Russell and WL Jamieson contributed equally to this study.
Received 23 June 2008; revised 11 August 2008; accepted 8 September 2008; published online 13 October 2008

Introduction

Solid tumors frequently colonize distant organs in a selective manner, a tissue tropism epitomized by the propensity of prostate adenocarcinoma to metastasize to the skeleton (Paget, 1889; Chambers *et al*., 2002). Patients with advanced prostate cancer frequently develop skeletal metastases and eventually succumb to them. Thus, the identification of factors responsible for promoting the colonization of the skeleton by malignant prostate phenotypes is paramount in establishing effective therapies to counteract metastatic complications of prostate adenocarcinoma. The survival and growth of cancer cells disseminated to the skeleton is considered dependent on trophic factors present in the bone marrow (Mundy, 2002; Fidler, 2003). It has been shown that bone-metastatic phenotypes produce molecules, such as parathyroid hormone-related peptide, which stimulate osteoblasts to release a receptor activator of nuclear factor-κB (RANKL), which in turn attracts and activates osteoclasts, thereby promoting osteolysis (Roodman, 2004). The degradation of bone matrix releases trophic factors, sustaining cancer cell proliferation and facilitating increased recruitment and activation of osteoclasts in a self-sustained vicious cycle, which may promote the expansion of the metastatic tumor mass within the bone tissue (Kingsley *et al*., 2007). Inhibition of osteoclast activity by administration of either bisphosphonates (Lee *et al*., 2002) or osteoprotegerin (Canon *et al*., 2008) limits the growth of cancer cells in the skeleton of animal models. These studies were conducted using bioluminescence and/or radiographic detection of bone lesions induced by intravascular injection or, more frequently, direct intraosseous implantation of cancer cells. However, at least 2×10^4 cells are needed in the bone to produce a detectable bioluminescent signal, which is visible not earlier than 2–3 weeks, following initial homing (Wetterwald *et al*., 2002; van der Pluijm *et al*., 2005). Analogously, radiographic analysis detects bone lesions produced by large numbers of cancer cells but is unable to identify single cancer cells or small foci (Fritz *et al*., 2007). Therefore, investigations of the interactions established by prostate cancer cells with the surrounding microenvironment soon after their extravasation into the bone marrow have been lacking.

It could be hypothesized that osteoclast recruitment in early metastatic stages may not occur due to the low number of cancer cells and the consequent paucity of secreted chemo-attractant and activating molecules. Thus, it is not until the tumor reaches a critical mass that such influence on the microenvironment is exerted. If this is the case, disseminated single cancer cells and small foci might rely on trophic molecules readily available in the bone marrow immediately after their arrival to ensure a successful lodging in the skeleton—before mutual interactions with osteoclasts can be established. The expression of receptors compatible with these trophic molecules would provide selected malignant phenotypes with a determinant survival advantage (Fidler, 2003).

In this study, we used an animal model of hematogenous skeletal metastases combined with a fluorescence-based histological analysis to monitor the establishment and progression of bone metastases from the arrival of individual cells to full-blown macroscopic tumors. Using this approach, we determined the spatial relationships between osteoclasts and micro-metastases and investigated the relevance of platelet-derived growth factor receptor-α (PDGFRα) expression for the survival and growth of prostate cancer cells in the bone marrow. Finally, we evaluated antibody-mediated targeting of PDGFRα as a strategy to counteract skeletal metastases from prostate cancer.

Results and discussion

In the first set of experiments, we investigated the involvement of osteoclasts in early skeletal micro-metastases. Male SCID mice were inoculated in the left cardiac ventricle with PC3-ML human prostate cancer cells, which consistently produce macroscopic metastases at the craniofacial region, tibia and femur of $\geqslant 80\%$ of animals within 4 weeks. The PC3-ML cells were previously selected from the widely used PC3 parental line for their invasive ability *in vitro* and metastatic potential *in vivo* (Wang and Stearns, 1991). We engineered these cells to stably express enhanced green fluorescent protein and, by the combined use of fluorescence stereomicroscopy, histological analysis and digital imaging of serial cryosections, identified small metastatic foci in the skeleton of mice at 1, 2 and 3 weeks following cell inoculation. A manual caliper was used to measure the volume of 4-week macro-metastases (Figure 1a). We found that metastases with a cross-section area of $28 \times 10^3\,\mu m^2$ or larger—which we usually observe 2 weeks after cell inoculation—were surrounded by an almost uninterrupted layer of osteoclasts, identified by TRAcP staining (Figure 1b). However, the smaller foci identified in the first 2 weeks after inoculation were found to be spatially unrelated to osteoclasts (Figure 1c and Supplementary Figure 1). Thus, our results indicate a later involvement of osteoclasts in metastatic progression and suggest the existence of mechanisms alternative to bone degradation to support the initial survival of prostate cancer cells in early bone micro-metastases. As osteoclast involvement appears to be a delayed event in metastatic progression, single cells and small foci would initially have to rely on the trophic support exerted by factors immediately available in the bone marrow stroma, through the stimulation of compatible cellular receptors. We have previously reported that PC3-ML cells express high levels of PDGFRα, a tyrosine-kinase receptor responsible for a strong *in vitro* activation of the PI3K/Akt survival pathway in response to human bone marrow (Dolloff *et al*., 2007). The PC3-N prostate cancer cells—a non-invasive counterpart of PC3-ML cells (Wang and Stearns, 1991)—express low levels of PDGFRα, whereas brain metastasis-derived DU-145 prostate cells lack this receptor (Dolloff *et al*., 2005). When exposed *in vitro* to human bone marrow, these cells show a modest or negligible activation of the PI3-K/Akt pathway, respectively (Dolloff *et al*., 2007). Inoculation of fluorescent DU-145 or PC3-N cells in SCID mice failed to produce macroscopic skeletal metastases after 4 weeks, in agreement with other studies (Wang and Stearns, 1991; Nemeth *et al*., 1999). However, we found that both PC3-N and DU-145 cells arrived at the skeleton with efficiency only slightly lower than PC3-ML cells (Table 1). All three cell types targeted the distal femur and proximal tibia, locating predominantly at the metaphysis and in close proximity of the growth plate (Figures 2a and b). The examination of tissue samples from the craniofacial region showed a preferential distribution of all three prostate cancer cell types to the teeth, indicating access to the mandible primarily through the dental pulp rather than bone marrow (Figure 4a). To assess the extravasation of cancer cells into the bone marrow stroma of femur and tibia, endothelial cells lining the marrow sinusoids were fluorescently labeled (Gupta *et al*., 2007). Twenty-four hours after their inoculation, the majority of cells were spatially located outside the sinusoids and in the bone marrow stroma (Figures 2c–e), in which they were still detected at 72 h post-inoculation (Table 1). Thus, despite their differing abilities in inducing macroscopic metastases, all three prostate phenotypes are able to arrive to the skeleton and extravasate, features we previously found might be related to the expression of the CX3CR1 chemokine receptor (Shulby *et al*., 2004; Jamieson *et al*., 2008). On the other hand, the inability of PC3-N and DU-145 cells to emulate the metastatic progression of PC3-ML cells could be correlated to their different patterns of PDGFRα expression, possibly leading to impaired survival following their extravasation into the bone marrow. To test this idea, mice were inoculated with fluorescent DU-145 or PC3-N cells and killed 1 week later. Neither cancer foci nor single cells could be detected in the femora or tibiae of mice inoculated with DU-145 cells, suggesting that these cells fail to survive between 72 h and 7 days after their arrival to the skeleton. Interestingly, although PC3-N cells did produce tumor foci, they were significantly smaller than those induced by PC3-ML cells after the same 1-week interval ($6.5 \pm 1.5 \times 10^2$ versus $19 \pm 5 \times 10^2\,\mu m^2$). The differences in PDGFRα expression observed among

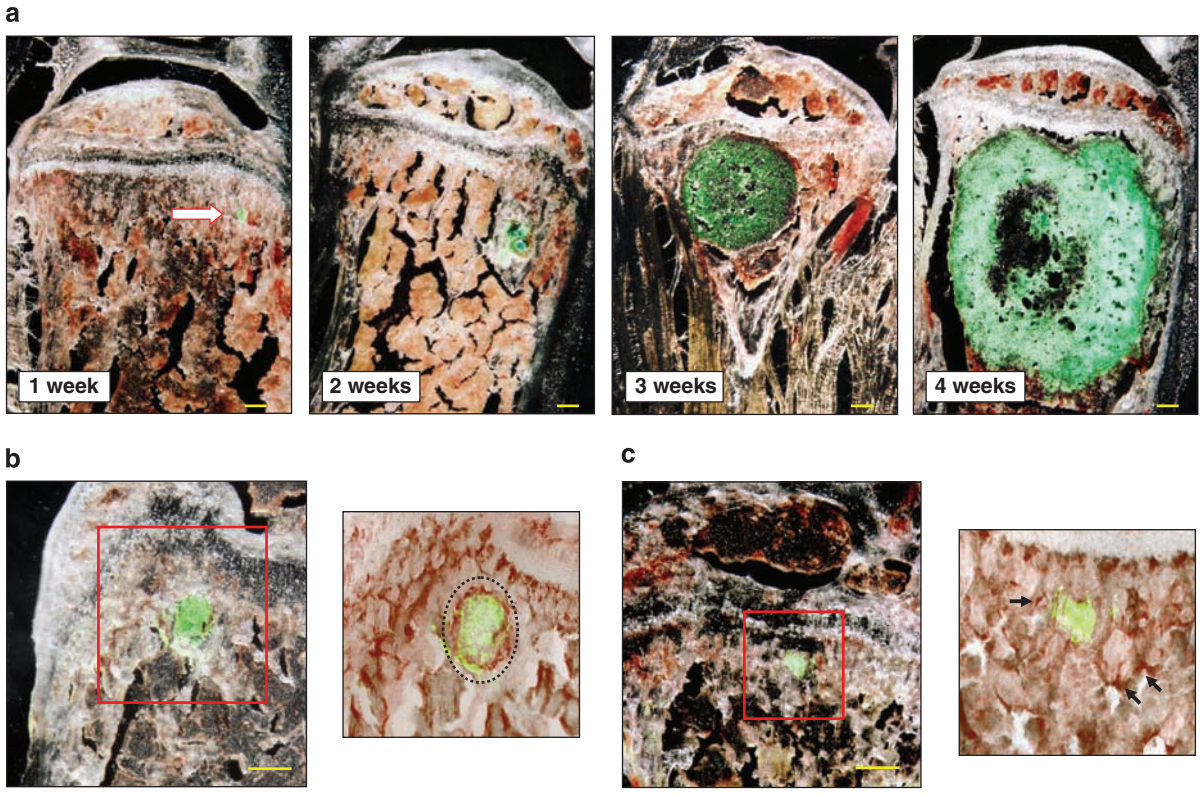

Figure 1 Progression of skeletal metastases from prostate cancer cells and spatial relationship with osteoclasts. (**a**) Enhanced green fluorescent protein-expressing human PC3-ML cells, inoculated in the left cardiac ventricle of SCID mice, locate to the upper tibia (shown) and lower femur in $\geqslant$80% of animals and progressively increase in size, measured by the calibrated digital analysis of fluorescence microscopy images (1 week: $1.9 \pm 0.5 \times 10^3\,\mu m^2$; 2 weeks: $35 \pm 6 \times 10^3\,\mu m^2$; 3 weeks: $264 \pm 60 \times 10^3\,\mu m^2$) or by a manual caliper (4 weeks: $14 \pm 4\,mm^3$). By the analysis of serial cryosections, the largest cross-section for each metastasis was identified, its relative length and width measured and the total area calculated using the ellipse formula: $l \times w \times 3.14$. Macroscopic metastatic tumors were measured by a caliper and their volume calculated by assimilating them to an ellipsoid using the formula: $l \times w^2 \times 0.52$ (Vantyghem *et al*., 2005). Bone tissue samples were fixed, decalcified and frozen. Serial cryosections were examined using a fluorescence stereomicroscope. Between 5 and 8 mice were used for the 1–3 week time points and 17 mice for the 4-week time points. The presence of active osteoclasts in the bone marrow regions colonized by cancer cells was histologically established by TRAcP staining. (**b**) Metastases with cross-section area larger than $28 \times 10^3\,\mu m^2$—indicated by the green fluorescent signal—were surrounded by an evident layer of active osteoclasts, as shown in the magnified panel; (**c**) smaller metastases were instead spatially unrelated to osteoclasts, which appear sparsely distributed (black arrows). Original magnifications: $\times$200 for (**a**) and $\times$400 for (**b** and **c**). Measurement bar is 100 μm.

Table 1 PC3-ML, PC3-N and DU-145 prostate cancer cells detected in the craniofacial region or femora and tibiae of mice inoculated 24 or 72 h earlier

	24 h		*72 h*	
	Mandible	*Legs*	*Mandible*	*Legs*
PC3-ML	13 ± 4	5 ± 2	29 ± 3	6 ± 1
PC3-N	12 ± 4	5 ± 1	10 ± 3	9 ± 2
DU-145	6 ± 2	5 ± 0.2	5 ± 2	2 ± 1

Five animals per group were used. A fluorescent stereomicroscope was used to examine all the serial cryosections obtained from each collected bone. The values indicate the average number of cells detected in either mandible or femora and tibiae combined.

the prostate cell lines tested in our study could mirror a comparable scenario *in vivo*. In fact, human arrays of malignant prostate tissue showed uniform and strong staining for PDGFRα combined with more heterogeneous expression patterns, often coexisting in the same gland (Figures 3a and b). We also consistently detected PDGFRα in human tissues of skeletal metastases from prostate adenocarcinoma (Figure 3c), which further implies a role for this receptor in the bone tropism of malignant prostate cells. Thus, the next series of experiments investigated whether an increase in PDGFRα expression could promote skeletal survival and growth of prostate cells originally lacking bone-metastatic potential. When PC3-N cells were stably transduced with the cDNA for human PDGFRα, they showed a significant increase in downstream Akt phosphorylation in response to PDGF-AA as compared to their wild-type counterparts (Figure 3d). We have previously described that human bone marrow aspirates are able to activate Akt in PC3-ML cells by recruiting PDGFRα (Dolloff *et al*., 2007). When PC3-N(PDGFRα) cells were tested upon similar conditions, we observed a phosphorylation of Akt comparable to that detected in PC3-ML cells (Figure 3e) as well as an evident PDGFRα phosphorylation (Figure 3f). As the newly obtained PC3-N(PDGFRα) cells showed signaling responses similar to the bone-metastatic

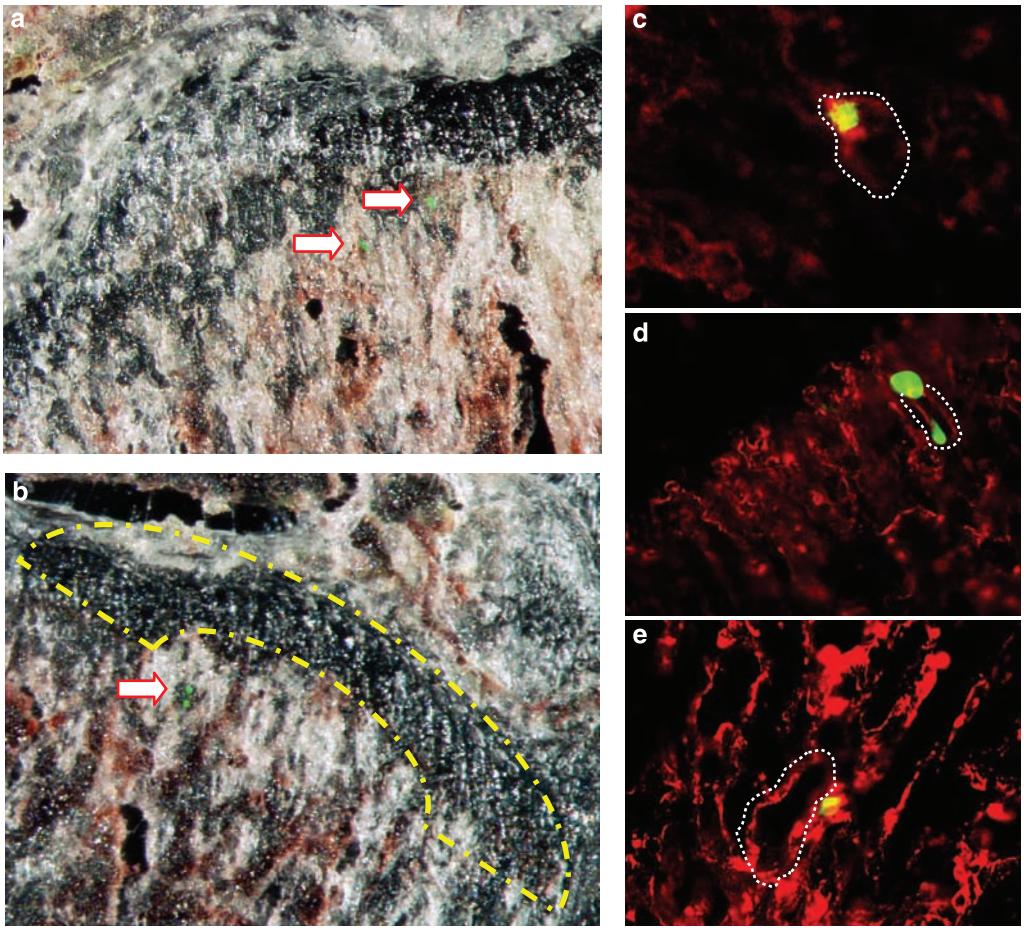

Figure 2 Early arrival of prostate cancer cells to the skeleton and extravasation in the surrounding stroma. (**a** and **b**) Fluorescent cells were detected in the femur and tibia of SCID mice at 24 or 72 h following inoculation in the left cardiac ventricle. Cancer cells (arrows) consistently located at the metaphysis and in the vicinity of the growth plate (yellow dashed line); the labeling of bone marrow sinusoids by a fluorescent lectin was used to establish the fraction of cancer cells that were (**c**) still in the vascular lumen as compared to cells (**d**) in the process of extravasating or (**e**) already migrated into the marrow's stroma. The white dotted line indicates the sectioned limits of three different bone marrow sinusoids. The ratios of cancer cells outside or inside the vasculature—24 h after inoculation—were 19 to 1 for PC3-ML cells (five positive sections from three mice), 12 to 0 for PC3-N cells (six positive sections from four mice) and 13 to 3 for DU-145 cells (12 positive sections from four mice).

PC3-ML cells, the next experiments aimed to determine their bone-metastatic potential. Thus, SCID mice were inoculated with either PC3-N (wt) or PC3-N(PDGFRα) cells, killed 3 weeks later and examined for fluorescent metastases in tibiae and femora. In contrast to PC3-N (wt) cells, which produced small metastases in only 2 of the 10 inoculated mice, the PC3-N(PDGFRα) cell induced evident bone tumors in 5 out of 7 mice (Figure 3g). Notably, PC3-N(PDGFRα) cells produced bone tumors comparable in size to those induced by PC3-ML cells after a similar 3-week interval (Figures 1 and 3h). Taken together, these results strongly support a determinant role for PDGFRα in the progression of prostate skeletal metastases in the skeleton. This effect would likely involve the down-stream stimulation of the PI3K/Akt pathway, which plays a central role in cellular survival and could support the trophism and proliferation of cancer cells (Carnero *et al*., 2008) before other tissue factors—such as those released from the bone matrix by osteoclasts at later stages of metastatic progression—become accessible. Notably, we have previously shown that human bone marrow can activate PDGFRα in a ligand-independent manner (Dolloff *et al*., 2007), termed transactivation, suggesting that the expression of this receptor might be determinant for the survival of cancer cells even in the absence of relevant levels of PDGF ligands in the marrow micro-environment. On the basis of this model, targeting PDGFRα could therefore impair the bone-metastatic potential of prostate cancer cells. To examine this possibility, we used the humanized monoclonal antibody IMC-3G3, which will soon begin phase-II trials. It has been previously shown (Loizos *et al*., 2005)—and further confirmed by our data (Supplementary Figure 2)—that IMC-3G3 is specific for human PDGFRα and does not affect the mouse form of the receptor. After cell inoculation, mice were randomly assigned to control (saline treated) or

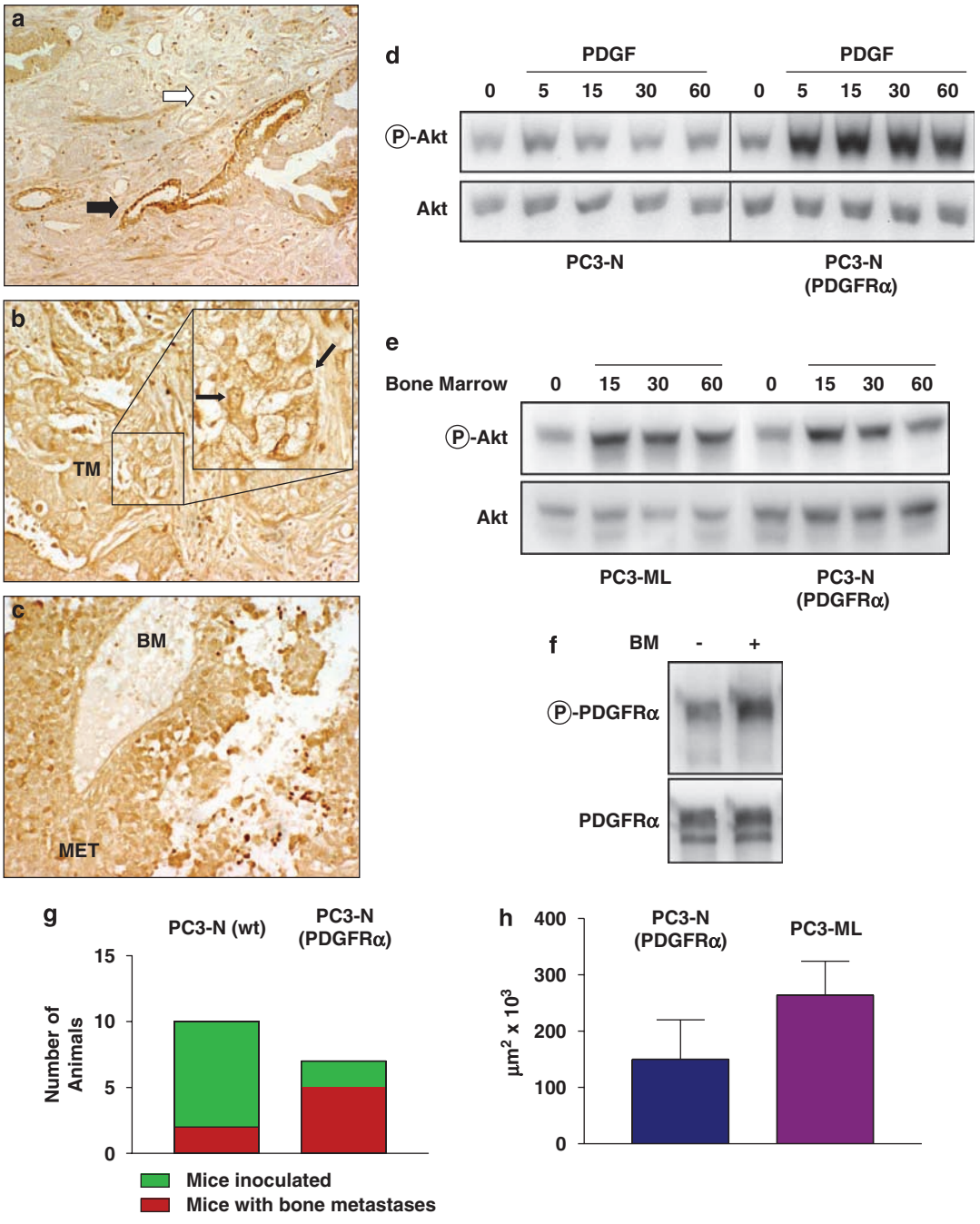

Figure 3 Human tissue arrays staining for platelet-derived growth factor receptor-α (PDGFRα) and induction of ectopic expression of PDGFRα in prostate cancer cells. (**a**) Dishomogeneous detection of PDGFRα in prostate adenocarcinoma, emphasized by positive (black arrow) and negative (white arrow) staining of two different gland acini; (**b**) homogeneous detection of PDGFRα. The expression of this receptor on the surface of prostate epithelial cells is confirmed by the peripheral staining shown in the magnified panel; (**c**) skeletal metastases from prostate adenocarcinoma also stain positive for PDGFRα, whereas bone marrow (BM) stains negative for the receptor. Staining intensity was scored based on a scale in which negative specimens were graded (0), tissue prevalently negative for PDGFRα showing some areas of positive staining were scored as (0–1) and tissue showing uniform staining for PDGFRα were scored as either (1–2) or (2–3) based on the intensity of the signal observed. Of the 105 cores of malignant human prostate tissue examined, 37 were scored as (0), 40 as (0–1), 22 as (1–2) and 6 as (2–3); (**d**) the overexpression of PDGFRα in PC3-N cells causes a dramatic increase of Akt phosphorylation in response to PDGF-AA; (**e**) PC3-N(PDGFRα) and PC3-ML cells—exposed to human bone marrow after being serum-starved for 4 h—phosphorylate Akt to a comparable degree in a time-dependent manner; (**f**) phosphorylation of PDGFRα in PC3-N(PDGFRα) cells exposed for 30 min to human bone marrow; (**g**) dramatic increase in the number of bone metastases observed after 3 weeks in tibiae and femora of mice inoculated with PC3-N(PDGFRα) cells (5 of 7 mice) as compared to PC3-N(wild-type) cells (2 of 10 mice); (**h**) comparable size of skeletal tumors induced by PC3-N(PDGFRα) and PC3-ML cells 3 weeks after intracardiac inoculation in mice ($150 \pm 70 \times 10^3$ and $263 \pm 60 \times 10^3$ μm^2, respectively (*t*-test; $P = 0.27$).

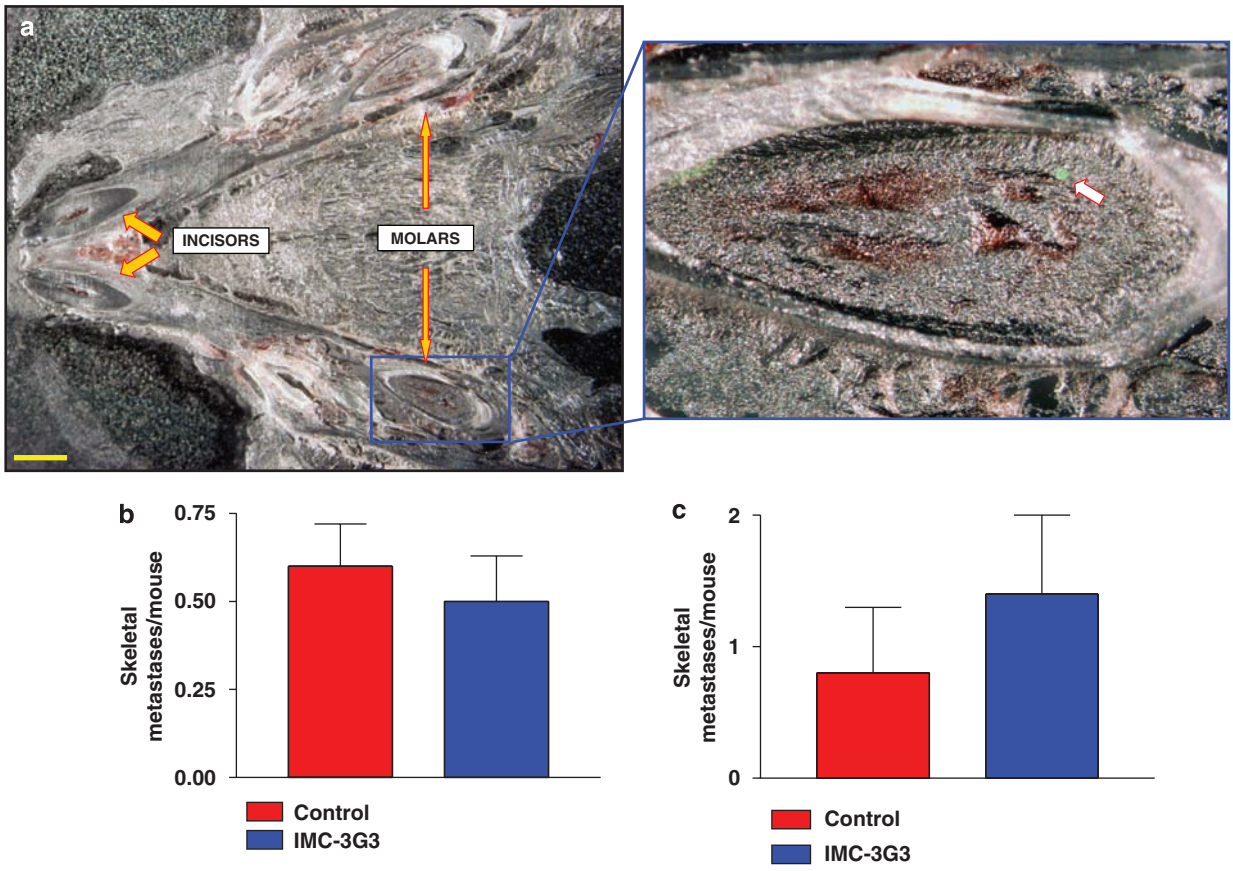

Figure 4 Arrival of prostate cancer cells to the mandible and effect of the immuno-mediated targeting of platelet-derived growth factor receptor-α (PDGFRα) in a mouse model. Prostate cancer cells show initial homing to the teeth before gaining access to the craniofacial region. (**a**) Transverse section of the mandible of a mouse inoculated in the left cardiac ventricle with fluorescent PC3-ML prostate cancer cells. The magnified panel shows a single cancer cell located in the dental pulp of a molar tooth. The administration of the humanized monoclonal antibody IMC-3G3 against PDGFRα did not affect the number of metastatic tumors in the mandible at (**b**) 2 or (**c**) 4 weeks following cancer cell inoculation. Original magnification: ×70. Measurement bar is 600 μm.

IMC-3G3-treated groups and killed 4 weeks later. The analysis of femora and tibiae showed 72% reduction in the number of macroscopic metastases observed in mice treated with IMC-3G3 (0.23 ± 0.1 tumor per animal) as compared to control groups (0.82 ± 0.2 tumor per animal). Most importantly, a much larger fraction of IMC-3G3-treated mice were free of metastases in either femur or tibia as compared to control animals (10 of 13 for IMC-3G3 versus 5 of 17 for controls) (Figure 5a). To ascertain whether IMC-3G3 exerts its effect in early stages of metastatic progression, subsequent experiments were conducted with inoculated animals randomly assigned to control or IMC-3G3 groups and killed after only 2 weeks. Similarly to what was observed after 4 weeks of IMC-3G3 treatment, the blockade of PDGFRα reduced the number of skeletal micrometastases in femora and tibiae by 70% (5.2 ± 1.2 per animal and 1.6 ± 0.7 per animal for saline and IMC-3G3, respectively) (Figure 5b). The larger number of cancer foci detected at 2 weeks compared to that of macroscopic metastases observed at 4 weeks—in both control and IMC-3G3 treated mice—is most likely the result of multiple foci coalescing into a single macrometastasis. The few metastases that progressed despite IMC-3G3 treatment appeared to elude an early effect, as they did not differ in size when compared to lesions observed in saline-treated animals ($354 \pm 60 \times 10^2$ versus $323 \pm 119 \times 10^2$ μm^2, respectively). Taken together, these results indicate that the blockade of PDGFRα dramatically inhibits the occurrence of skeletal metastasis and its effect is predominantly exerted during the very initial stages of bone colonization by prostate cancer cells.

As mentioned above, prostate cancer cells locate to the teeth of inoculated mice before invading the bone tissue of the mandible (Figure 4a). Interestingly, IMC-3G3 did not affect the number or size of metastases in the craniofacial region after either 2 or 4 weeks of treatment (Figures 4b and c). Differences between bone marrow and dental pulp, such as the presence of unique trophic factors sustaining the continuous dental eruption in rodents, may explain a more prevailing role of PDGFRα in the survival of prostate cancer cells in long bones, which are by far more common sites of metastasis than the craniofacial region in prostate adenocarcinoma patients (Schneider *et al*., 2005).

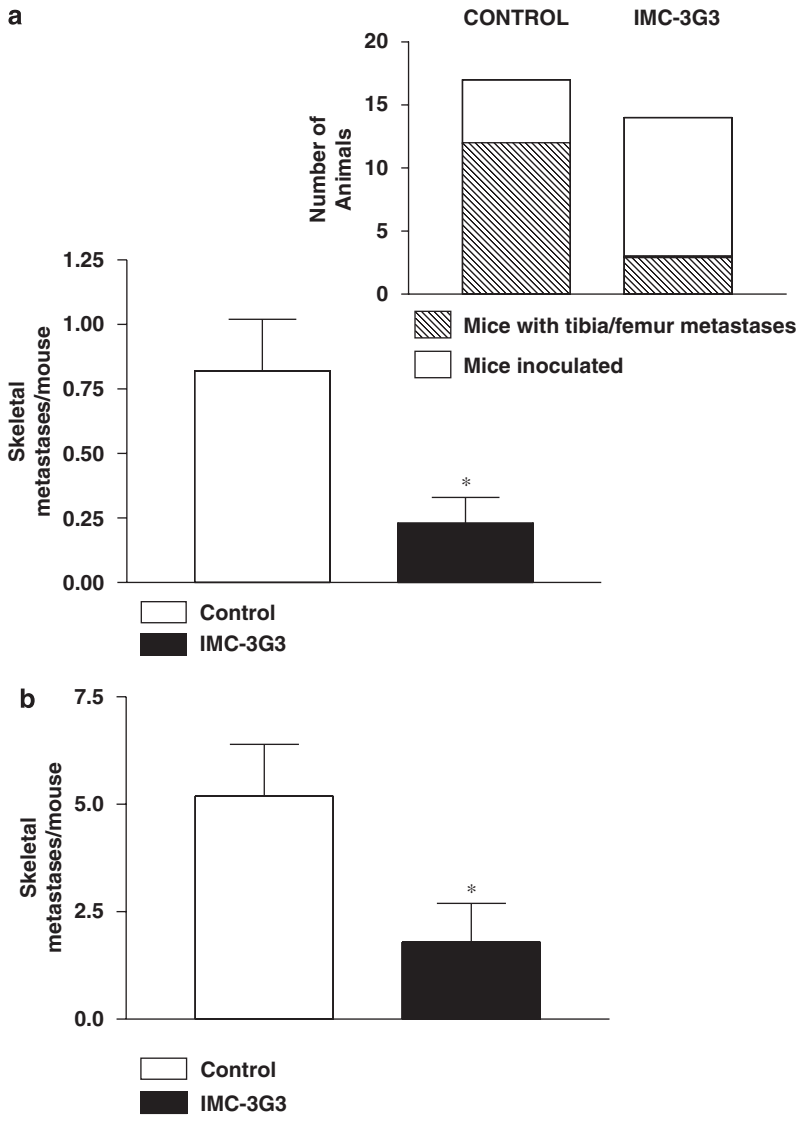

Figure 5 Immuno-mediated targeting of platelet-derived growth factor receptor-α (PDGFRα) inhibits skeletal metastases at femora and tibiae in a mouse model. (**a**) Targeting PDGFRα dramatically reduces the number of skeletal macro-metastases in the leg by 76%, as shown by IMC-3G3 administered to SCID mice inoculated in the left cardiac ventricle with PC3-ML prostate cancer cells and killed 4 weeks later (*t*-test; $P=0.015$). The inset shows the number of control and IMC-3G3-treated mice inoculated with PC3-ML cells as well as the significantly higher number of animals free from femur and tibia macro-metastases observed in the IMC-3G3-treated group (5 of 17 for control group and 10 of 13 for IMC-3G3-treated group). The correct execution of cell inoculation in mice free of metastases in femur and tibia was confirmed by the presence of metastases in the craniofacial region and/or adrenal glands; (**b**) administration of IMC-3G3 reduced femur and tibia micro-metastases by 70% as compared to control groups in mice killed 2 weeks following cancer cell inoculation. (*t*-test; $P=0.038$).

In summary, our study differentiates the role of osteoclasts in early- and late-stage metastases and provides the first compelling evidence for a central role of PDGFRα in defining a bone-metastatic prostate cancer phenotype. The translation of these observations to the clinic is reflected by the ability of the humanized monoclonal antibody IMC-3G3 to significantly reduce—and in most cases impede—the establishment and progression of skeletal micro-metastases in our animal model.

Recent clinical trials using imatinib mesylate (STI571, Gleevec), a small-molecule inhibitor of PDGFRs—either alone (Mathew *et al*., 2004; Rao *et al*., 2005; Lin *et al*., 2006; Bajaj *et al*., 2007) or in combination with docetaxel (Mathew *et al*., 2007)—have been disappointing, showing significant adverse toxic effects combined with lack of efficacy in counteracting bone metastatic progression and/or improving overall survival. However, it should be considered that, although in the adult organism both PDGFRα and PDGFRβ cooperate in modulating largely overlapping physiological process—including angiogenesis, wound healing and tissue homeostasis (Heldin and Westermark, 1999; Betsholtz, 2004)—PDGFRβ plays an overall predominant role (Andrae, Gallini and Betsholtz, 2008). Also, experiments in mice showed that the intracellular domain of PDGFRβ could fully substitute for the PDGFRα, whereas replacement of PDGFRβ cytoplasmic domain

with that of the α-receptor caused abnormalities in vascular smooth muscle cell development and function, among others (Yarden *et al*., 1986). Thus, the indiscriminate blockade of both PDGFRα and PDGFRβ by imatinib might be responsible for the systemic adverse effects observed in clinical trails. On the other hand, the selective inactivation of PDGFRα—using a monoclonal antibody rather than a broad-range inhibitor—could limit the survival of malignant cells that depend on this receptor while causing limited toxicity, due to the largely duplicate physiological roles exerted by PDGFRβ.

Furthermore, the preclinical animal studies conducted to investigate the effects of imatinib were based on bone tumors mostly produced by implanting large numbers of prostate cancer cells directly in the tibia. Although significantly shortening the time required for each experiment, this approach inherently bypasses the initial stages of establishment and progression while focusing on macroscopic bone lesions with characteristics of late metastases. Thus, the different histopathological features of intra-osseous inoculation of cancer cells in the animal as compared to human skeletal metastases—combined with the late timing of therapeutic intervention—might also explain the disappointing effects of imatinib in clinical trials.

Our results indicate that the inhibition of PDGFRα is very effective during the initial stages of metastatic progression. Only 15% of men currently present with macroscopic metastases when first diagnosed with primitive prostate cancer (Ross *et al*., 2006). Thus, one can envision a prophylactic strategy targeting PDGFRα in prostate cancer patients positive for this receptor that are metastasis-free at diagnosis or after initial therapy as well as patients with advanced disease harboring occult metastases.

Materials and methods

Cell lines and cell culture

All cell lines were cultured at 37 °C and 5% CO_2 in Dulbecco's modified Eagle's medium supplemented with 10% fetal bovine serum (Hyclone, Logan, UT, USA) and 0.1% gentamicin (Invitrogen, Carlsbad, CA, USA). Cells were engineered to stably express enhanced green fluorescent protein by transduction with a proprietary lentiviral vector (America Pharma Source, Bethesda, MD, USA) in complete culture medium for 24 h using a multiplicity of infection of 50 i.f.u. per cell.

Cell inoculation

Five-week-old male immunocompromised SCID mice (CB17-SCRF, Taconic, Germantown, NY, USA) were housed in a germ-free barrier. At 6 weeks of age, animals were anesthetized with ketamine (80 mg/kg) and xylazine (10 mg/kg) and inoculated in the left cardiac ventricle with cancer cells (5×10^4 in 100 μl of serum-free Dulbecco's modified Eagle's medium/F12 using a 30-gauge needle). All experiments were conducted in accordance with NIH guidelines for the humane use of animals. All protocols involving the use of animals were approved by the Drexel University College of Medicine Committee for the Use and Care of Animals.

Ectopic PDGFRα expression

Human PDGFRα (NM_006206) was expressed in the same lentiviral vector (America Pharma Source) used to obtain stably fluorescent cells. The PDGFRα cDNA was originally expressed in a PCDNA3.1 vector (Invitrogen) and had been cloned in using a newly introduced 5′-*Bam*H1 site and an existing 3′ *Bam*H1 site. To clone it into the lentiviral vector, we introduced a 5′ *Bam*H1 and a 3′ *Xho*1 site by PCR using the following primers: *Bam*H1: 5′-GGATCCCAGAG CTATGGGGA-3′, *Xho*I: 5′-CTCGAGGTGGCCCCAGAAG T-3′. Cells were transduced using a multiplicity of infection of 50 i.f.u. per cell. As the lentiviral vector contains an enhanced green fluorescent protein-IRES site, the cells expressing PDGFRα were isolated and purified by flow cytometry and sorting based on their fluorescence intensity.

Human bone marrow acquisition and processing

The bone marrow samples from normal male donors (ages 18–45) were supplied by Lonza Biosciences (Poietics Donor Program, Walkersville, MD, USA). Samples were shipped and maintained at 4 °C throughout processing and were subsequently stored at −80 °C. Briefly, samples were centrifuged at 1500 r.p.m. to separate the soluble and cellular phases. Supernatant was removed and filtered using 0.8 and 0.22 μm filters in succession.

In vitro *experimental protocol*

Cells were starved from serum for 4 h before being exposed to bone marrow or PDGF-AA (20 ng/ml). Fifty micro-liters of processed bone marrow were administered to cells in 1 ml of experimental medium for a final 1:20 dilution.

SDS–polyacrylamide gel electrophoresis and western blotting

Cell lysates were obtained and SDS–polyacrylamide gel electrophoresis and western blot analysis were performed as previously described (Shulby *et al*., 2004), with few modifications. Membranes were blotted with antibodies targeting phospho-Akt (Ser-473, Cell Signaling Technology, Danvers, MA, USA), PDGFRα (R&D Systems, Minneapolis, MN, USA) and total Akt (Cell Signaling, Danvers, MA). Primary antibody binding was detected using an horseradish peroxidase-conjugated secondary antibody (Pierce, Rockford, IL, USA). Chemiluminescent signals were obtained using SuperSignal West Femto reagents (Pierce) and detected with the Fluorochem 8900 imaging system and relative software (Alpha Innotech, San Leandro, CA, USA). Densitometry analysis was performed using the UN-SCAN IT software (Silk Scientific). Samples were run on the same gels for effective comparison of intensity levels. Each experiment was repeated at least three times and provided similar results.

Detection of PDGFRα phosphorylation

Cells were washed twice with ice-cold phosphate-buffered saline and lysed with immunoprecipitation buffer (50 mM Tris, 150 mM NaCl, 10 mM NaF, 10 mM sodium pyrophosphate, 1% NP40) supplemented with protease and phosphatase inhibitors (Protease Inhibitor Cocktail Set III, Phosphatase Inhibitor Cocktail Set II, Calbiochem, Gibbstown, NJ, USA). Cell lysates (750 μg) were incubated with agarose-conjugated anti-PDGFRα primary antibody (Santa Cruz, Santa Cruz, CA, USA) overnight at 4 °C. Immunoprecipitation was carried out according to the manufacturer's protocol, with immunoprecipitated protein run on a 4–12% polyacrylamide gel (Lonza Biosciences, Walkersville, MD, USA). Western blotting was carried out as previously described using an antibody directed against phosphotyrosine (Cell Signaling). Even loading was confirmed by stripping the membrane and blotting for total PDGFRα.

Tissue preparation
Bones and soft-tissue organs were collected and fixed in 4% formaldehyde solution. Bones were decalcified in 0.5 M EDTA for 7 days followed by incubation in 30% sucrose. Tissues were frozen in O.C.T. medium (Electron Microscopy Sciences, Hatfield, MA, USA) by placement over dry-ice chilled 2-methylbutane (Fisher, Pittsburgh, PA, USA). Serial sections of 80 μm in thickness were obtained using a Microm HM550 cryostat (Mikron, San Marcos, CA, USA).

Histology
TRAcP staining Slides were incubated at 37 °C for 5 min in a solution containing naphthol AS-BI phosphate and ethylene glycol monoethyl ether (Sigma, St Louis, MO, USA). Slides were then transferred to a solution containing sodium nitrite and pararosaniline chloride (Sigma) for approximately 3 min.

Evaluation of cell extravasation Tissues were fixed in ice-cold acetone and then treated with 2 μg/ml biotinylated lycopersicon esculentum lectin (Vector Laboratories, Burlingame, CA, USA) for 1 h at room temperature to label the endothelial cells of the bone marrow sinusoids. After washing in Tris-buffered saline, tissues were incubated at room temperature for 1 h in 1.8 μg/ml of CY3-conjugated streptavidin (Jackson Immunoresearch, West Grove, PA, USA). An average of 20 cryosections were obtained from the mandible and legs of animals killed at either 24 or 72 h post-inoculation and examined for fluorescent cancer cells. Digital images were captured, processed for the removal of background fluorescence, and the spatial relationships of green-fluorescent cancer cells with the red-fluorescent bone marrow sinusoids were determined. The total numbers of cells located within the red-fluorescent rim of the sinusoids (intra-vascular), overlapping with it (in the process of extravasating) or located outside the red-fluorescent rim (fully extravasated) were counted.

PDGFRα immunostaining Human tissue microarrays PR951, PR208, PR803 and GL802 were obtained from US Biomax Inc. (Rockville, MD, USA) Tissue samples were deparaffinized with Histosolve (Dako Cytomation, Carpinteria, CA, USA) and re-hydrated with decreasing concentrations of ethanol. Endogenous peroxidase was quenched using methanol and hydrogen peroxide. Antigen retrieval was performed using Dako Cytomation Target Retrieval Solution in a 95 °C water bath for 30 min. Arrays were blocked with 10% normal donkey serum in Tris-buffered saline for 60 min, then incubated in horseradish peroxidase-conjugated IMC-3G3 (10 μg/ml) in blocker overnight at 4 °C. Antibody binding was visualized with a chromogenic DAB kit (Vector, Burlingame, CA, USA). Slides were dehydrated with increasing concentrations of ethanol, cleared in Histosolve and mounted using Permount. The IMC-3G3 antibody was conjugated to horseradish peroxidase using EZ-Link Plus Activated Peroxidase kit (Pierce), according to the manufacturer's instructions. The specificity of the IMC-3G3 antibody for the PDGFRα was validated using human tissue arrays containing tissue cores of 35 cases of glioblastoma (highly expressing the receptor; Thorarinsdottir *et al*., 2008) and 5 cases of normal brain tissue (weakly positive for the receptor).

Microscopy and measurements
Bright-field and fluorescence images of single cells, small foci and macroscopic metastases were acquired using an SZX12 Olympus stereomicroscope coupled to an Olympus DT70 CCD color camera. Digital images were analysed with ImageJ software (http://rsb.info.nih.gov/ij/) and calibrated by obtaining a pixel to millimeter ratio.

IMC-3G3 administration
Animals received a loading dose of 214 mg/kg immediately after inoculation with PC3-ML cells, followed by a maintenance dose of 60 mg/kg every 72 h thereafter. Doses and administration schedule were selected based on tumor-growth inhibitory studies and pharmacokinetic analyses conducted by ImClone Systems Inc. Control animals received comparable volumes of sterile phosphate-buffered saline solution.

Statistics
We analysed number and size of skeletal metastases in control and IMC-3G3-treated groups using a two-tailed Student's *t*-test. A value of $P \leqslant 0.05$ was considered statistically significant.

Acknowledgements

The cDNA for human PDGFRα was a kind gift of Dr Carl-Henrik Heldin (Ludwig Institute for Cancer Research, Uppsala, Sweden). We thank Dr Olimpia Meucci (Department of Pharmacology and Physiology) for critically reading the manuscript and helpful discussion, Dr Mark Stearns (Department of Pathology and Laboratory Medicine) for helpful discussion, Dr Gregg Johannes (Department of Pathology and Laboratory Medicine) for help with the PDGFRα-expressing vector, Mr Michael Amatangelo for his contribution to the immuno-detection of PDGFRα in human tissues and Dr Nick Loizos (ImClone Systems Inc., New York, NY, USA) for kindly providing the IMC-3G3 antibody. This study was supported in part by the NIH Grant GM067892 to AF.

References

Andrae J, Gallini R, Betsholtz C. (2008). Role of platelet-derived growth factors in physiology and medicine. *Genes Dev* **22**: 1276–1312.

Bajaj GK, Zhang Z, Garrett-Mayer E, Drew R, Sinibaldi V, Pili R *et al*. (2007). Phase II study of imatinib mesylate in patients with prostate cancer with evidence of biochemical relapse after definitive radical retropubic prostatectomy or radiotherapy. *Urology* **69**: 526–531.

Betsholtz C. (2004). Insight into the physiological functions of PDGF through genetic studies in mice. *Cytokine Growth Factor Rev* **15**: 215–228.

Canon JR, Roudier M, Bryant R, Morony S, Stolina M, Kostenuik PJ *et al*. (2008). Inhibition of RANKL blocks skeletal tumor progression and improves survival in a mouse model of breast cancer bone metastasis. *Clin Exp Metastasis* **25**: 119–129.

Carnero A, Blanco-Aparicio C, Renner O, Link W, Leal JF. (2008). The PTEN/PI3K/AKT signalling pathway in cancer, therapeutic implications. *Curr Cancer Drug Targets* **8**: 187–198.

Chambers AF, Groom AC, MacDonald IC. (2002). Dissemination and growth of cancer cells in metastatic sites. *Nat Rev Cancer* **2**: 563–572.

Dolloff NG, Russell MR, Loizos N, Fatatis A. (2007). Human bone marrow activates the Akt pathway in metastatic prostate cells through transactivation of the alpha-platelet-derived growth factor receptor. *Cancer Res* **67**: 555–562.

Dolloff NG, Shulby SS, Nelson AV, Stearns ME, Johannes GJ, Thomas JD *et al*. (2005). Bone-metastatic potential of human prostate cancer cells correlates with Akt/PKB activation by alpha platelet-derived growth factor receptor. *Oncogene* **24**: 6848–6854.

Fidler IJ. (2003). The pathogenesis of cancer metastasis: the 'seed and soil' hypothesis revisited. *Nat Rev Cancer* **3**: 453–458.

Fritz V, Louis-Plence P, Apparailly F, Noël D, Voide R, Pillon A *et al*. (2007). Micro-CT combined with bioluminescence imaging: a dynamic approach to detect early tumor-bone interaction in a tumor osteolysis murine model. *Bone* **40**: 1032–1040.

Gupta GP, Ngyuen DX, Chiang AC, Bos PD, Kim JY, Nadal C *et al*. (2007). Mediators of vascular remodeling co-opted for sequential steps in lung metastasis. *Nature* **446**: 765–770.

Heldin C-H, Westermark B. (1999). Mechanism of action and *in vivo* role of platelet-derived growth factor. *Physiol Rev* **79**: 1283–1316.

Jamieson WL, Shimizu S, D'Ambrosio JA, Meucci O, Fatatis A. (2008). CX3CR1 is expressed by prostate epithelial cells and androgens regulate the levels of CX3CL1/fractalkine in the bone marrow: potential role in prostate cancer bone tropism. *Cancer Res* **68**: 1715–1722.

Kingsley LA, Fournier PG, Chirgwin JM, Guise TA. (2007). Molecular biology of bone metastasis. *Mol Cancer Ther* **10**: 2609–2617.

Lee YP, Schwarz EM, Davies M, Jo M, Gates J, Shang X *et al*. (2002). Use of zoledronate to treat osteoblastic versus osteolytic lesions in a severe-combined-immunodeficient mouse model. *Cancer Res* **62**: 5564–5570.

Lin AM, Rini BI, Weinberg V, Fong K, Ryan CJ, Rosenberg JE *et al*. (2006). A phase II trial of imatinib mesylate in patients with biochemical relapse of prostate cancer after definitive local therapy. *BJU Int* **98**: 763–769.

Loizos N, Xu Y, Huber J, Liu M, Lu D, Finnerty B *et al*. (2005). Targeting the platelet-derived growth factor receptor α with a neutralizing human monoclonal antibody that inhibits the growth of tumor xenografts: implications as a potential therapeutic target. *Mol Cancer Ther* **4**: 369–379.

Mathew P, Thall PF, Bucana CD, Oh WK, Morris MJ, Jones DM *et al*. (2007). Platelet-derived growth factor receptor inhibition and chemotherapy for castration-resistant prostate cancer with bone metastases. *Clin Cancer Res* **13**: 5816–5824.

Mathew P, Thall PF, Jones D, Perez C, Bucana C, Troncoso P *et al*. (2004). Platelet-derived growth factor receptor inhibitor imatinib mesylate and docetaxel: a modular phase I trial in androgen-independent prostate cancer. *J Clin Oncol* **22**: 3323–3329.

Mundy GR. (2002). Metastasis to bone: causes, consequences and therapeutic opportunities. *Nat Rev Cancer* **2**: 584–593.

Nemeth JA, Harb JF, Barroso Jr U, He Z, Grignon DJ, Cher ML. (1999). Severe combined immunodeficient-hu model of human prostate cancer metastasis to human bone. *Cancer Res* **59**: 1987–1993.

Paget S. (1889). The distribution of secondary growths in cancer of the breast. *Lancet* **1**: 571–573.

Rao K, Goodin S, Levitt MJ, Dave N, Shih WJ, Lin Y *et al*. (2005). A phase II trial of imatinib mesylate in patients with prostate specific antigen progression after local therapy for prostate cancer. *Prostate* **62**: 115–122.

Roodman GD. (2004). Mechanisms of bone metastasis. *N Engl J Med* **350**: 1655–1664.

Ross RW, Oh WK, Hurwitz M, D'Amico AV, Richie JP, Kantoff PW. (2006). Neoplasm of the prostate. In: Holland-Frei (ed). *Cancer Medicine*. BC Decker Inc. publisher, pp 1431–1461.

Schneider A, Kalikin LM, Mattos AC, Keller ET, Allen MJ, Pienta KJ *et al*. (2005). Bone turnover mediates preferential localization of prostate cancer in the skeleton. *Endocrinology* **146**: 1727–1736.

Shulby SA, Dolloff NG, Stearns ME, Meucci O, Fatatis A. (2004). CX_3CR1-fractalkine expression regulates cellular mechanisms involved in adhesion, migration, and survival of human prostate cancer cells. *Cancer Res* **64**: 4693–4698.

Thorarinsdottir HK, Santi M, McCarter R, Rushing EJ, Cornelison R, Jales A *et al*. (2008). Protein expression of platelet-derived growth factor receptor correlates with malignant histology and PTEN with survival in childhood gliomas. *Clin Cancer Res* **14**: 3386–3394.

van der Pluijm G, Que I, Sijmons B, Buijs JT, Lowik CW, Wetterwald A *et al*. (2005). Interference with the microenvironmental support impairs the *de novo* formation of bone metastases *in vivo*. *Cancer Res* **65**: 7682–7690.

Vantyghem SA, Allan AL, Postenka CO, Al-Katib W, Keeney M, Tuck AB *et al*. (2005). A new model for lymphatic metastasis: development of a variant of the MDA-MB-468 human breast cancer cell line that aggressively metastasizes to lymph nodes. *Clin Exp Metastasis* **22**: 351–361.

Wang M, Stearns ME. (1991). Isolation and characterization of PC-3 human-prostatic tumor sublines which preferentially metastasize to select organs in SCID mice. *Differentiation* **48**: 115–125.

Wetterwald A, van der Pluijm G, Que I, Sijmons B, Buijs J, Karperien M *et al*. (2002). Optical imaging of cancer metastasis to bone marrow: a mouse model of minimal residual disease. *Am J Pathol* **160**: 1143–1153.

Yarden Y, Escobedo JA, Kuang WJ, Yang-Feng TL, Daniel TO, Tremble PM *et al*. (1986). Structure of the receptor for platelet-derived growth factor helps define a family of closely related growth factor receptors. *Nature* **323**: 226–232.

Supplementary Information accompanies the paper on the Oncogene website (http://www.nature.com/onc)